Energy Proceedings
Vol 53, 2025
ISSN 2004-2965

Numerical evaluation of melting of phase change materials in two-dimensional rectangular vessels with different aspect ratios under vibration conditions#

Qi Deng[1], Hua Chen[1], Wen-long Cheng[1,*]
1 Department of Thermal Science and Energy Engineering, University of Science and Technology of China, Hefei, Anhui, PR China
Correspond author: e-mail: wlcheng@ustc.edu.cn (Wen-long Cheng).

ABSTRACT

The vibration phenomenon widely existing in engineering is often ignored when considering the effect of the aspect ratio of the container on the melting of phase change material (PCM). In this paper, a melting model of PCM in a two-dimensional rectangular container with constant temperature boundary and variable length is constructed, and the influence of rectangular aspect ratio (AR) on the melting process of PCM under vibration is studied by numerical calculation. Our findings reveal that at a static state, larger aspect ratios enhance natural convection within the vessel, thereby modestly accelerating PCM melting. Paradoxically, this also leads to increased paraffin content, prolonging the melting of the contracting solid phase. However, when subjected to vibrations, every aspect ratio experiences an accelerated melting process, with the enhancement more pronounced at higher vibration frequencies. For example, when frequency is 5Hz, melting time in vessel (AR=0.4) is 2.4% shorter than static, while (AR=2) vessel's time is 7% shorter. Notably, the larger aspect ratio vessels exhibit a more significant acceleration with frequency increase. Furthermore, the average Nusselt number during melting oscillates periodically with vibration, consistently exceeding its static-state counterpart.

Keywords: energy storage, rectangular vessel, phase change material melting, vibrate, aspect ratio

NONMENCLATURE

Abbreviations	
PCM	Phase change material
RT-27	phase change point of about 27 ℃
Symbols	
C	Mushy zone constant, kg/(m^3·s)
c_p	Specific heat, J/(kg·K)
g	Gravitational acceleration, m/s^2
h	Sensible enthalpy, J/kg
ΔH	Latent enthalpy, J/kg
L_m	Latent heat fusion, J/kg
p	Pressure, Pa
S	source term [kg/m^2·s^2]
T_l	Liquid phase temperature point, ℃
T_s	Solid phase temperature point, ℃
α	Thermal expansion coefficient, 1/K
γ	liquid phase fractions
κ	Thermal conductivity, W/(m·K)
ρ	Density, kg/m^3

1. INTRODUCTION

With the development of society and science and technology, the contradiction between chemical energy use and environmental pollution is becoming more and more acute, and there is an urgent need for the application of energy storage technology to alleviate the spatial and temporal mismatch between the supply and demand of new energy use. In recent years, latent heat energy storage[1] represented by phase change materials has received widespread attention. Phase change materials have the advantages, such as high enthalpy of phase change, chemical stability. Because of these benefits, phase change materials have a wide range of applications, including thermal energy storage and thermal management[2]. However, the limited thermal conductivity of solid-liquid phase change materials, restricts their ability to respond quickly to temperature changes. The researchers discovered that modifying the container's form can effectively enhance phase-change material heat transmission.

The shape and size[3][4][5] of the vessel mainly affect the formation and development of natural convection during PCM melting. Brent et al.[6] first simulated the melting and convection process of pure gallium metal in a rectangular vessel and found that the method can accurately predict the shape and location of the solid-liquid interface during the melting process.

This is a paper for the 16th International Conference on Applied Energy (ICAE2024), Sep. 1-5, 2024, Niigata, Japan.

Later, the melting process of PCM in a rectangular vessel gradually attracted the attention of researchers.

The aspect ratio of the rectangle is also an important factor affecting the melting process in a rectangular vessel[7]. Xie et al. [8] took the two-dimensional rectangular cavity PCM with constant volume and constant heat flux as the research object, and studied the influence of aspect ratio and heating wall on the melting behavior of PCM. The results showed that the complete melting time increased with the increase of aspect ratio.

However, most studies on the aspect ratio of melting ignore the vibration, which is common in engineering and affecting the melting of phase-change materials[9][10]. In this paper, A vibration-based melting model for phase change material in a two-dimensional rectangular container with a constant temperature and a variable length boundary is constructed. And the effect of aspect ratio on the phase change material in a rectangular vessel under vibration is investigated by numerical methods, and the influence mechanism of aspect ratio and vibration is analyzed.

2. MODEL DESCRIPTION

2.1 *Physical model*

The two-dimensional model depicted in Fig. 1 utilizes Paraffin RT-27[11][12] as PCM, initialized at 300 K (thermophysical properties detailed in Table.1). The rectangular region's base is fixed at 30mm, with varying aspect ratios achieved by adjusting side wall heights (12mm, 21mm, 30mm, 60mm, corresponding to ratios 0.4, 0.7, 1, 2). In this scenario, the amount of paraffin corresponding to each unit length of the heating wall remains consistent across all containers. The heated wall on the right maintains 353.15 K. Past researchers have hardly used this type of boundary condition. Other walls are adiabatic and non-slip. This configuration ensures uniform paraffin wax per unit length along the heating wall. The physical model is illustrated in Fig. 1.

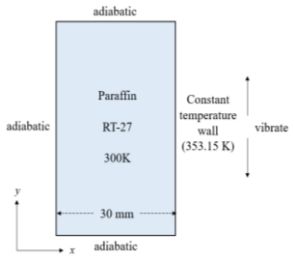

Fig.1 Physical model

$$aspect\ ratio\ (AR) = \frac{side\ wall}{bottom\ wall} \tag{1}$$

Table.1 Thermophysical properties of RT-27

Properties	PA-RT27
Solid density ($\mathbf{kg/m^3}$)	870
Paste density ($\mathbf{kg/m^3}$)	870-760 Linear
Therm. cond. (Solid) ($\mathbf{W/m \cdot K}$)	0.24
Therm. Cond. (Liquid) ($\mathbf{W/m \cdot K}$)	0.15
Liquid density ($\mathbf{kg/m^3}$)	$\frac{760}{(1+\beta(T-T_l))}$
Solid specific heat ($\mathbf{J/kg \cdot K}$)	2400
Liquid specific heat ($\mathbf{J/kg \cdot K}$)	1800
Dynamic viscosity ($\mathbf{kg/m \cdot s}$)	3.42×10^{-3}
Latent heat ($\mathbf{J/kg}$)	179000
Solid melt temperature (℃)	301.15
Liquid temperature (℃)	303.15
Thermal expansion coefficient ($\mathbf{K^{-1}}$)	0.5×10^{-3}

To simplify the calculations, the following assumptions are made about the model:

1) Liquid-phase PCM is Newtonian fluid and incompressible, and the flow process is laminar with no viscous dissipation

2) The volume change during the phase change of PCM is neglected;

3) The physical parameters of the paste region vary linearly with temperature;

4) Boussinesq approximation is used for the density change due to thermal expansion of fluid phase change materials, and the relation is:

$$\rho = \frac{\rho_l}{1+\alpha(T-T_l)} \tag{2}$$

2.2 *Governing equation*

The enthalpy method is used to solve the melting process of PCM. The enthalpy-based equation for the melting process of PCM taking into account the natural convection and vibration caused by the density difference due to temperature is given below:

$$\frac{\partial \rho}{\partial t} + \nabla \cdot (\rho \vec{u}) = 0 \tag{3}$$

$$\frac{\partial (\rho \vec{u})}{\partial t} + \nabla \cdot (\rho \vec{u}\vec{u}) = -\nabla p + \nabla \cdot (\mu \nabla \vec{u}) + \rho \vec{F} + \vec{S} \tag{4}$$

$$\frac{\partial (\rho H)}{\partial t} + \vec{u} \cdot \nabla (\rho H) = \nabla \cdot (\kappa \nabla T) \tag{5}$$

Where $\vec{u}$ can be divided into x (u) and y (v) directions and F is generated by gravity and vibration together, and the vibration displacement equation is:

$$Y = Asin(2\pi ft)$$

$$F = g\left[1 + \frac{A \cdot (2\pi f)^2}{|g|}\sin(2\pi ft)\right] \quad (6)$$

Where f is the vibration frequency (Hz), A is the amplitude (m), and g is the acceleration of gravity. H is computed as the sum of the sensible and latent enthalpy

$$H = h + \Delta H \quad (7)$$

$$h = h_{ref} + \int_{T_{ref}}^{T} c_p dT \quad (8)$$

$$\Delta H = \gamma L_m \quad (9)$$

$$\gamma = \begin{cases} 0 & T < T_s \\ \dfrac{T - T_s}{T_l - T_s} & T_s < T < T_l \\ 1 & T > T_l \end{cases} \quad (10)$$

$\vec{S}$ can be divided into two parts: the horizontal direction (u) and the vertical direction (v). S_u and S_v are the momentum source terms

$$S_u = \frac{(1-\gamma)^2}{\gamma^3 + \varepsilon} A_{mush} \cdot u \quad (11)$$

$$S_v = \frac{(1-\gamma)^2}{\gamma^3 + \varepsilon} A_{mush} \cdot v - \frac{\rho_l g}{1 + \alpha(T - T_l)} \quad (12)$$

Where A_{mush} and γ are paste region constants and liquid phase fractions, respectively. The paste region constant is between 10^4 and 10^7 and is commonly used to calculate the melting rate of PCM in molten pastes. In this study, 10^5 is considered to be a suitable value for the mushy region constant [13].

$$A_{mush} = -C\frac{(1-\gamma)^2}{\gamma^3 + \varepsilon} \quad (13)$$

For solid state PCM(γ=0), to avoid being divided by zero, ε is introduced, which is a smaller value of 0.001.

2.3 *Vibration model*

The equation of vibration velocity obtained from displacement equation is

$$v_y = \frac{dY}{dt} = 2\pi f A sin(2\pi ft) \quad (14)$$

The fixed amplitude is A=2.5×10^{-5}m. In this study, four different frequencies are selected: *f*=2, 3, 4, 5 Hz.

3. NUMERICAL PROCEDURE AND VALIDATION

3.1 *Numerical procedures and validation*

In this paper, Fluent software is used for numerical computation. PISO algorithm is used and the coupling between pressure and momentum is done using implicit solution format. The momentum equation is discretized using the second-order windward format and the pressure for the continuity equation is corrected using the PRESTO format. The subrelaxation factors for pressure, density, momentum, and liquid-phase fraction are 0.3, 0.4, 0.4, and 0.5, respectively. Scaled absolute residuals of 10^{-3}, 10^{-3}, and 10^{-6} are set as the convergence criteria for the continuity, velocity component and energy, respectively. The number of iterations is set to 30 for each time step setting and the convergence of the solution is checked at each time step.

3.2 The grid independence study and time step independence study

Select a rectangular structure with an aspect ratio of 2 for validation. Four sets of structure grids (13850, 20500, 29200, 46120) and three set of time step (0.01s,0.02s,0.05s) are generated. After the grid independence and time step independence study, the setting with a grid number of 29200 and a time step of 0.02s is finally adopted.

3.3 The validation study

Referring to the experimental and modeling parameters in the reference of J. Vogel et al [14]. The thermophysical parameters of the eutectic mixture of 54 wt% KNO_3 and 46 wt% $NaNO_3$ used in the experiments are shown in Table.2. One side of the wall is heated at a constant temperature of 232 ℃ and the rest of the walls are adiabatic. Numerical calculations without vibration are performed based on the mathematical-physical model developed in this paper and Fluent setup. Fig.2 shows the comparison of the numerical predictions with the liquid phase fraction in reference under the same parameters and conditions. The trend of the numerical simulation results remains consistent with a maximum error of less than 10%. Therefore, the validity of the numerical model in this paper can be verified.

Table.2 Thermophysical properties of KNO_3-$NaNO_3$

Material property	KNO_3-$NaNO_3$
Solid density (kg/m^3)	2050
Liquid density (kg/m^3)	1959
Heat capacity (Liquid) ($J/kg \bullet K$)	1492
Heat capacity (Solid) ($J/kg \bullet K$)	1350
Thermal conductivity ($W/m \bullet K$)	0.46
Melting point (℃)	219.5
Latent heat (kJ/kg)	94
Thermal expansion coefficient ($1/K$)	3.5×10^{-4}

Dynamic viscosity (Pa • s)	5.8×10^{-3}

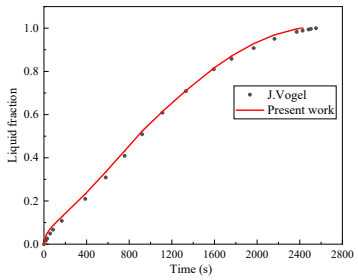

Fig.2 Comparison of liquid phase fraction curves

4 RESULTS AND DISCUSSIONS

In this section, the melting process of PCM in a vessel with different aspect ratios is studied numerically at static and at different vibration frequencies (f =2, 3, 4, 5Hz). The melting time of PCM, average Nusselt number, and maximum fluid velocity are analyzed to reveal the mechanism of the effect of vibration on the melting rate and heat transfer efficiency of PCM in vessels with different aspect ratios.

4.1 *Melting process in a vessel with various aspect ratios without vibration*

Fig.3 shows the melting process of paraffin in a rectangular vessel. At the beginning of melting, the form of heat transfer in this period is dominated by heat conduction. As melting progresses, the liquid adjacent to the heated wall becomes sufficiently warm, initiating natural convection within the vessel. Fueled by thermal buoyancy, this liquid rises along the heated wall, traverses the phase interface to transmit heat, descends to the container's base for reheating, and repeats the cycle. This combined conduction-convection phase, known as the mixing stage, dominates heat transfer. The melting front steadily advances towards the vessel's upper left corner, entering the slowly diminishing solid phase called shrink solid, which persists until complete melting is achieved.

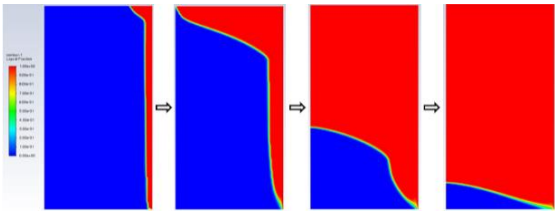

Fig.3 The melting process of paraffin

Fig.4 shows the variation of liquid phase fraction with time in the vessel for each aspect ratio. It can be seen that the time required for melting increases with the increase of aspect ratio. The Nusselt number during melting for each aspect ratio vessel is shown in Fig.5(a). The Nusselt number of the vessels with larger aspect ratio is overall smaller than the vessels with smaller aspect ratio. When the Nusselt number decreases in the middle and late stages of melting, it decreases more slowly for the vessels with larger aspect ratio. The maximum velocity in a vessel with different aspect ratio at a static state is shown in the Fig.5(b). Vessels with a higher aspect ratio offer an extended natural convection path, resulting in enhanced flow rates and intensified convection. Although this larger interface and convection strength expedite melting, the increased paraffin mass necessitates longer solid-phase shrinkage, ultimately prolonging the overall melting time for larger aspect ratio containers.

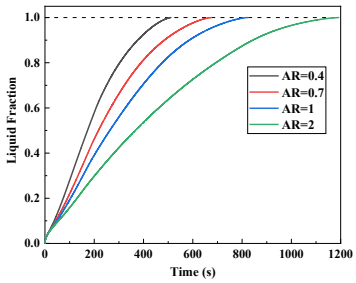

Fig.4 The change process of liquid fraction in a vessel with different aspect ratio at a static state

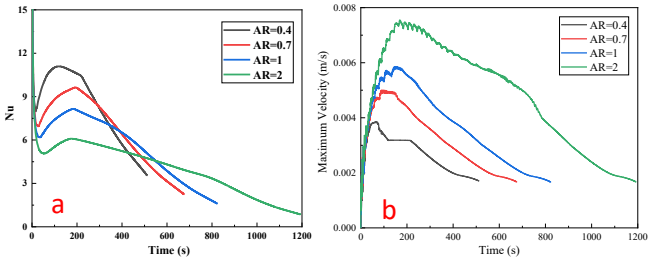

Fig.5 (a) Change of Nusselt number in a rectangular container at static; (b) Change in maximum velocity in the container at a static state.

4.2 Melting process in a vessel with various aspect ratios with vibration

Figure 6(a) illustrates the ratio of melting times under vibration to stationary conditions for PCMs in containers of varying aspect ratios at each frequency. For paraffin waxes, despite limited influence from low vibration frequency and amplitude on overall liquid phase fraction changes, vibration accelerates the total

melting time to a certain degree, particularly in large aspect ratio containers. As frequency increases, this acceleration effect becomes more pronounced, notably reducing melting time in large aspect ratio vessels. For instance, in the AR=2 vessel, Fig.6(b) depicts the liquid phase fraction variation over time, consistently higher in the vibrating state compared to the stationary state at any given moment.

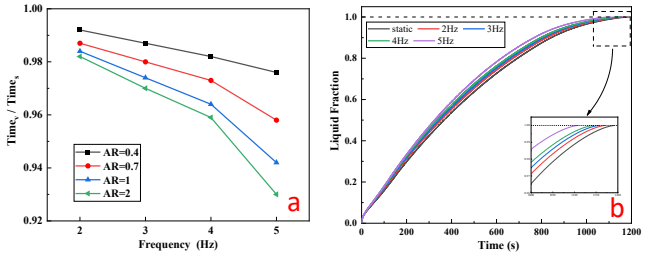

Fig.6 (a) The ratio of melting time under vibration to melting time at static state for each aspect ratio vessel; (b) variation of liquid phase fraction of paraffin in vessel with time at different vibration frequencies

Taking the case of vibration frequency of 5Hz as an example. The Nusselt number in the container of each aspect ratio is shown in Fig.7, In the early stage of melting, the Nusselt number of each aspect ratio in the vibration case is larger than that of the stationary state, and the later stage is slightly smaller than that of the stationary state. The Nusselt number in the vibration case are with the vibration cycle of small fluctuations, the overall trend is similar to the stationary state. For instance, in the AR=0.7 vessel, the comparison between the maximum speed in the container with each aspect ratio under vibration and the static state is shown in the Fig.8. The maximum flow velocity under vibration is often greater than that at static, indicating that vibration promotes the strength of natural convection. This continued until the late melting period, when the strength of the natural convection weakened and the speed gradually became similar. Vibration is an up and down periodic movement in the Y direction. While at static, the maximum velocity in the container is located at the top of the natural convection path near the side wall, and the velocity direction is generally upward. Therefore, the maximum velocity affected by vibration shows an irregular periodic change.

The reason for the above phenomenon is that the vibration strengthens the intensity of natural convection and promotes the mixing of the paste-like region near the phase interface, which enhances the heat transfer efficiency. The natural convection path in the container with a large aspect ratio is longer, and the vibration has a more obvious effect on the strengthening of natural convection, and the melting interface in the container with a high aspect ratio is also longer, and the vibration promotes the mixing of the paste region near the long melting interface, which accelerates the melting rate in this region. The combined effect of the two accelerates the melting process in the rectangular vessel at the first level of greater acceleration in the high aspect ratio vessel.

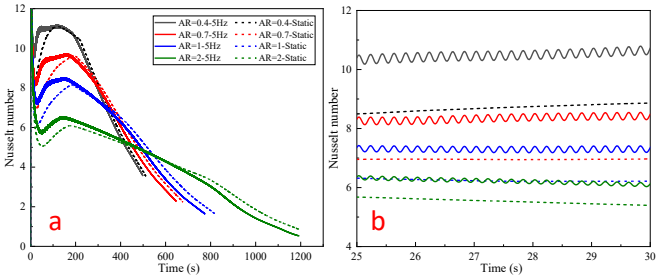

Fig.7 (a) Variation of Nusselt number in vessels with different aspect ratios at a static state and under vibration(5Hz); (b) Enlarged view from 25 to 30 seconds in Fig.7 (a).

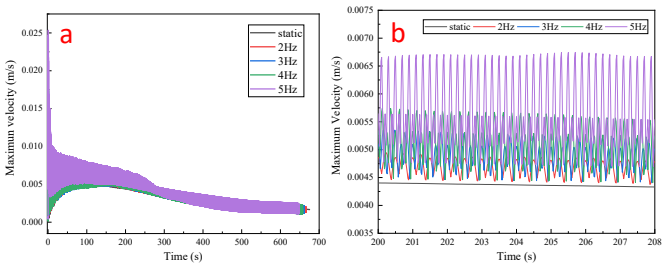

Fig.8 (a) Variation of maximum velocity in vessels with different aspect ratios at a static state and under vibration(5Hz); (b) Enlarged view from 200 to 208 seconds in Fig.8 (a).

CONCLUSIONS

This paper delves into the melting dynamics of PCMs with varying aspect ratios under vibration. We scrutinize how these ratios and vibration frequencies influence the melting process. By analyzing the liquid-phase fraction evolution and average Nusselt number, we compare and contrast the melting behavior under vibrational and non-vibrational conditions.

The results are as follows:

(1) An increase in aspect ratio promotes the initial stages of paraffin melting. However, a larger aspect ratio

means more paraffin, which takes more time in the solid phase of contraction, thereby significantly increasing the overall melting time.

(2) Vibration favorably reduces melting time of phase change materials by intensifying natural convection during melting and augmenting heat transfer in the paste zone. This acceleration becomes increasingly evident with rising frequency.

(3) Vessels with larger aspect ratios exhibit a heightened sensitivity to vibration during paraffin melting, with the enhancement effect intensifying for higher aspect ratios and frequencies.

(4) The average Nusselt number in the rectangular vessel under vibration varies periodically with vibration, and is significantly larger than the average Nusselt number at a static state and decreases more slowly in the rapid melting phase of the pre-melting stage.

ACKNOWLEDGMENT

This work was supported by the National Key R&D Program of China (Grant No. 2022YFC2204403), the National Natural Science Foundation of China (Grant No. 46652376153) and Major Science and Technology Project of Anhui Province (Grant No. 202203a07020023).

REFERENCES:

[1] J. Wang, X. Liu, U. Desideri. Performance improvement evaluation of latent heat energy storage units using improved bi-objective topology optimization method. Applied Energy, Volume 364, 2024, 123131

[2] J. Kang, Q. Deng, H. Liu, H, Chen, R. Zhao, C. Peng, X. Zhao, W. Cheng. Study on Temperature Noise Suppression Characteristics Based on Multilayer Composite Structure. Int J Thermophys 45, 109 (2024)

[3] Z. Qin, C. Ji, Z. Low, W. Tong, C. Wu, F. Duan. Geometry effect of phase change material container on waste heat recovery enhancement. Applied Energy, Volume 327, 2022, 120108

[4] R. Ge, Q. Li, C. Li, Q. Liu. Evaluation of different melting performance enhancement structures in a shell-and-tube latent heat thermal energy storage system. Renewable Energy, Volume 187,2022, Pages 829-843

[5] Z. Wang, Y. Li, Y. Wang, A. Li. Stagewise melting heat transfer characteristics of phase change material in a vertically placed rectangular enclosure. Journal of Energy Storage, Volume 62,2023,106917

[6] A.D. Brent, V.R. Voller, K.J. Reid. Enthalpy-porosity technique for modeling convection-diffusion phase change: application to the melting of a pure metal. Numer. Heat Transf. Part A: Appl.13 (1988)pp. 297-318.

[7] S. Huang, J. Lu, Y. Li, L. Xie, L. Yang, Y. Cheng, S. Chen, L. Zeng, W. Li, Y. Zhang, L. Wang. Experimental study on the influence of PCM container height on heat transfer characteristics under constant heat flux condition. Applied Thermal Engineering, Volume 172,2020,115159

[8] S. Xie, W. Wu. Effect of aspect ratio on PCM melting behavior in a square cavity. International Communications in Heat and Mass Transfer. Volume 143, 2023, 106708.

[9] S. Zeng, S. Chen, G. Wu. Effect of inclination angle on melting process of phase change materials in a square cavity under mechanical vibration. Journal of Energy Storage, Volume 36, 2021, 102392

[10] N. Joshy, M. Hajiyan, A. Siddique, S. Tasnim, H. Simha, S. Mahmud. Experimental investigation of the effect of vibration on phase change material (PCM) based battery thermal management system. Journal of Power Sources, Volume 450, 2020, 227717

[11] M. ELIDI, M. KARKRI, M. TANKARI, S. VINCENT. Hybrid cooling based battery thermal management using composite phase change materials and forced convection. Journal of Energy Storage, Volume 41, 2021, 102946

[12] M. Bechiri, K. Mansouri. Study of heat and fluid flow durin melting of PCM inside vertical cylindrical tube. International Journal of Thermal Sciences, Volume 135, 2019, Pages 235-246

[13] P. Biwole, P. Eclache, F. Kuznik. Phase-change materials to improve solar panel's performance. Energy and Buildings, Volume 62, 2013, Pages 59-67,

[14] J. Vogel, J. Felbinger, M. Johnson. Natural convection in high temperature flat plate latent heat thermal energy storage systems. Applied Energy, Volume 184, 2016, Pages 184-196